

Tuning the morphology to enhance the catalytic activity of α -Ag₂WO₄ through V-doping

K.L. Patrocinio¹, J.R. Santos¹, L.I. Granone², M.A. Ponce^{3,4}, M.S. Churio², L K. Ribeiro^{1,5}, M. D. Teodoro⁶, R. Llusrá⁵, J. Andrés^{5*}, E. Longo¹, M. Assis^{5,*}

¹CDMF-UFSCar, Universidade Federal de São Carlos, P.O. Box 676, CEP, 13565-905, São Carlos, SP, Brazil.

²Departamento de Química y Bioquímica, Facultad de Ciencias Exactas y Naturales, Instituto de Investigaciones Físicas de Mar del Plata (IFIMAR), CONICET, Universidad Nacional de Mar del Plata (UNMdP), Mar del Plata, 7600, Argentina.

³Instituto de Investigaciones en Ciencia y Tecnología de Materiales (INTEMA), Universidad Nacional de Mar del Plata (UNMdP), Mar del Plata, 7600, Argentina.

⁴Physics and Engineering Research Center CIFCEN (CICCPBA-CONICET), National University of the Center of the Province of Buenos Aires (UNCPBA), Tandil, B7000GHG, Argentina.

⁵Department of Analytical and Physical Chemistry, University Jaume I (UJI), Castelló, 12071, Spain.

⁶Department of Physics, Federal University of São Carlos, São Carlos, SP 13565-905, Brazil.

*Corresponding author: marcelostassis@gmail.com; andres@qfa.uji.es

Supporting Information

Refinement of Rietveld: Through the refinement (**Table 1**), the average crystallite size was obtained through the Scherrer equation (Eq. 1 and 2), using the FWHM of the most intense peak. The Scherrer equation is described by:

$$D = \frac{0.89\lambda}{(\beta \cos\theta)} \quad (\text{Eq. 1})$$

$$\beta = \sqrt{(\beta_{obs}^2 + \beta_{st}^2)} \quad (\text{Eq. 2})$$

where D is the average crystallite size, λ is the X-ray wavelength (0.15406 nm), β_{obs} is FWHM, β_{obs} is FWHM of LaB₆ standard and, θ is the Bragg angle. The lattice strain parameter can be obtained by Equation 3:

$$\epsilon = \frac{\beta}{(4 \tan\theta)} \quad (\text{Eq. 3})$$

GC detection: For the detection of methyl phenyl sulfone (Aldrich, CAS 3112-85-4, retention time (rt) = 3.9 s), 4-methoxyphenyl methyl sulfone (Aldrich, CAS 3517-90-6, rt = 5.0 s), 4-(methylsulfonyl)toluene (Aldrich, CAS 31855-99-7, rt = 4.5s) diethylsulfone (Aldrich, CAS 597-35-3, rt = 2.1s), 4-chlorophenyl methyl sulfone (Fisher Scientific,

CAS 98-57-7, rt = 4.6 s), and 1-(methylsulfonyl)-4-nitrobenzene (Fisher Scientific, CAS 2976-30-9, rt = 4.8 s) the main oven temperature was initially held at 75°C for 2 min and then increased at a rate of 20°C /min to 325°C, where it was maintained for 2 min. For the detection of diphenyl sulfone (Aldrich, CAS 127-39-9, rt = 5.7 s) the main oven temperature was initially held at 40°C for 2 min and then increased at a rate of 5°C/min to 325 °C, where it was maintained for 2 min. The method-specific parameters were as follows: inlet temperature, 325 °C; sample injection volume of 1 µL with split injector mode; carrier gas N₂. Data processing was performed using the OpenLab 3.5 software provided by Agilent. As initial reagents, thioanisole (Aldrich, CAS 100-68-5, rt = 2.2 s), 4-methoxythioanisole (Aldrich, CAS 3517-90-6, rt = 5.2 s), 4-methyl p-tolyl sulfide (Aldrich, CAS 623-13-2, rt = 2.7 s), diethylsulfide (Aldrich, CAS 352-93-2, rt = 1.7 s), 4-chlorothioanisol (Fisher Scientific, CAS 123-09-1, rt= 3.1 s), diphenyl sulfide (Aldrich, CAS 139-66-2, rt = 21.8 s), and 4-nitrothioanisole (Aldrich, CAS 701-57-5, rt = 3.9 s).

Table SI-1. Comparison of the amount in mol of V (%) added to the nominal and real a-AW crystal lattice.

Sample	[V] nominal (%)	[V] real (%)
AW	0.0000	0.0000
AW1V	0.0100	0.0092
AW2V	0.0200	0.0210
AW4V	0.0400	0.0438

Table SI-2. Lattice parameters and unit cell volumes obtained by Rietveld refinement for the samples.

Sample	R _{wp} (%)	R _p (%)	X ²	a (Å)	b (Å)	c (Å)	V (Å ³)	FWHM (°)	ε	D (nm)
AW	11.26	8.60	1.369	10.81(2)	11.95(1)	5.85(5)	756.53(8)	0.465	0.651	18.559
AW1V	9.91	7.73	1.128	10.88(2)	12.04(4)	5.90(8)	774.43(8)	0.379	1.542	22.758
AW2V	10.18	7.98	1.437	10.88(5)	12.04(2)	5.90(6)	774.12(3)	0.323	1.919	26.723
AW4V	9.94	7.82	1.305	10.89(1)	12.04(3)	5.90(1)	774.10(1)	0.389	1.233	22.163
CIF	-	-	-	10.887	12.040	5.907	774.290	-	-	-
Calc.	-	-	-	11.127	12.335	5.825	799.518	-	-	-

Table SI-3. Comparison between experimental and active theoretical Raman modes of this study and the literature.

Mode	This work		Literature			Longo et al. ⁴ (theoretical)
	Experimental	Theoretical	Sreedevi et al. ¹	Pereira et al. ²	Pinatti et al. ³	
A_{1g}	-		44	-	-	40.4
A_{1g}	-		60	60	59	54.1
B_{1g}	-		92	82	81	87
A_{2g}	102		116	116	114	112.2
A_{2g}	171		182	179	179	152.4
A_{1g}	-		208	206	204	212.4
B_{1g}	-		248	249	249	246.2
A_{2g}	307		306	306	301	308.6
B_{2g}	333		336	338	-	329.6
A_{2g}	375		366	368	365	369.5
B_{2g}	-		488	486	-	450.8
B_{2g}	-		510	508	-	523.4
B_{2g}	-		546	-	-	564.2
A_{1g}	579		590	586	584	599.4
B_{1g}	-		629	-	-	628.6
B_{1g}	665		667	669	662	662.8
B_{1g}	-		730	728	-	712.7
B_{2g}	741		754	759	755	716.6
A_{1g}	773		778	778	777	809.0
A_{2g}	-		800	805	801	813.5
A_{1g}	875		884	884	881	845.3

Table SI-4. Comparison between the values of Surface energy (E_{surf} , eV), contribution of surface area by total area (C_i , %) and Polyhedron energy ($E_{\text{polyhedron}}$, eV) for each α -AW and α -AWV morphology.

Surface	α -AW Ideal	A	B	α -AW rod-like	α -AW cobblestone-like
[010]	0.20(52.5)	0.60(16.4)	1.11(4.23)	1.41(7.35)	1.41(6.62)
[100]	0.38(27.6)	0.70(0.00)	0.70(0.00)	0.70(0.00)	0.20(46.7)
[001]	0.53(19.9)	0.20(37.6)	0.20(32.4)	0.20(19.7)	0.20(46.7)
[110]	0.65(0.00)	0.73(4.91)	0.85(10.6)	2.00(0.00)	2.00(0.00)
[101]	0.68(0.00)	0.33(41.1)	0.27(52.7)	0.23(72.9)	0.40(0.00)
[011]	0.83(0.00)	0.83(0.00)	0.83(0.00)	0.83(0.00)	0.83(0.00)
$E_{\text{polyhedron}}$	0.31	0.34	0.34	0.31	0.28

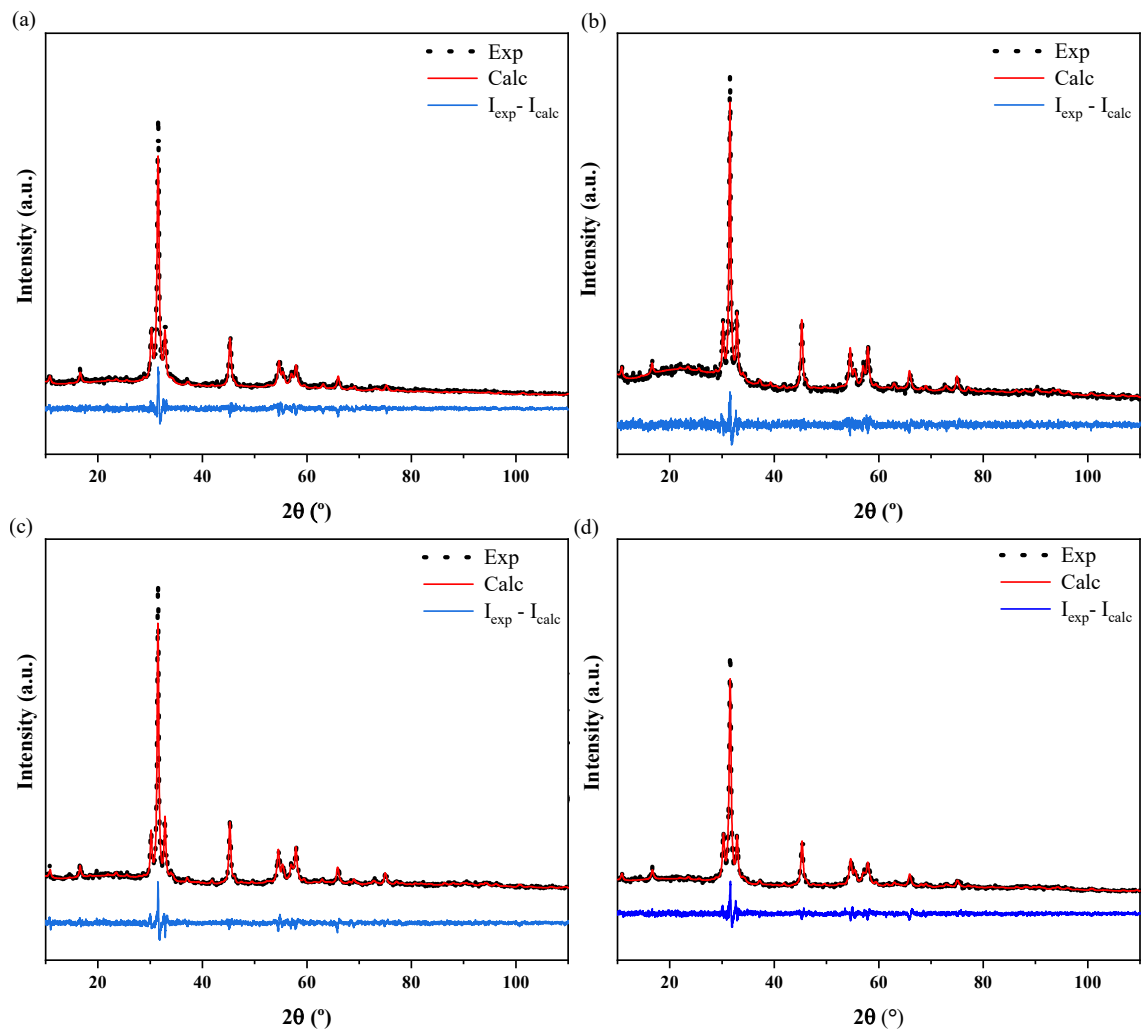
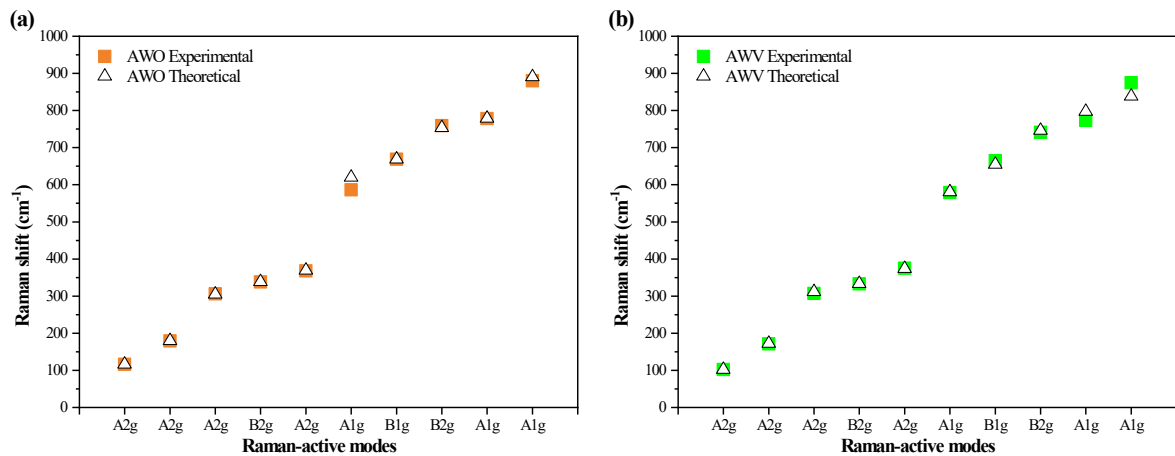


Figure SI-1. Rietveld refinement plot for AW (a), AW1V (b), AW2V (c) and AW4V (d),



microcrystals obtained by the CP method at 70 °C for 20 min.

Figure SI-2. Comparison between the relative positions of theoretical and experimental Raman-active modes: Raman spectra of the (a) AW pure and (b) doped with vanadium.

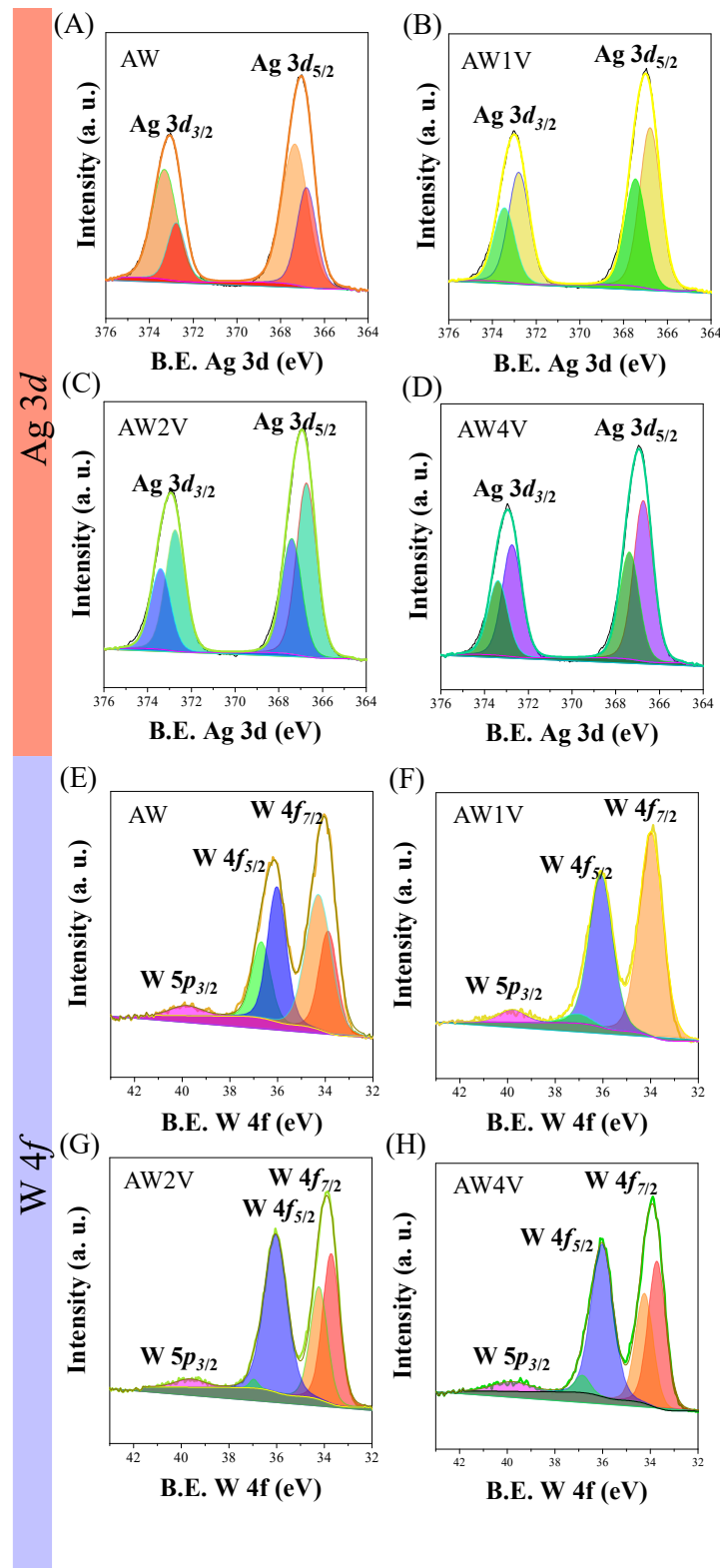


Figure SI-3. Core-level XPS spectra of Ag 3d (a-d) and W 4f for the samples(e-h).

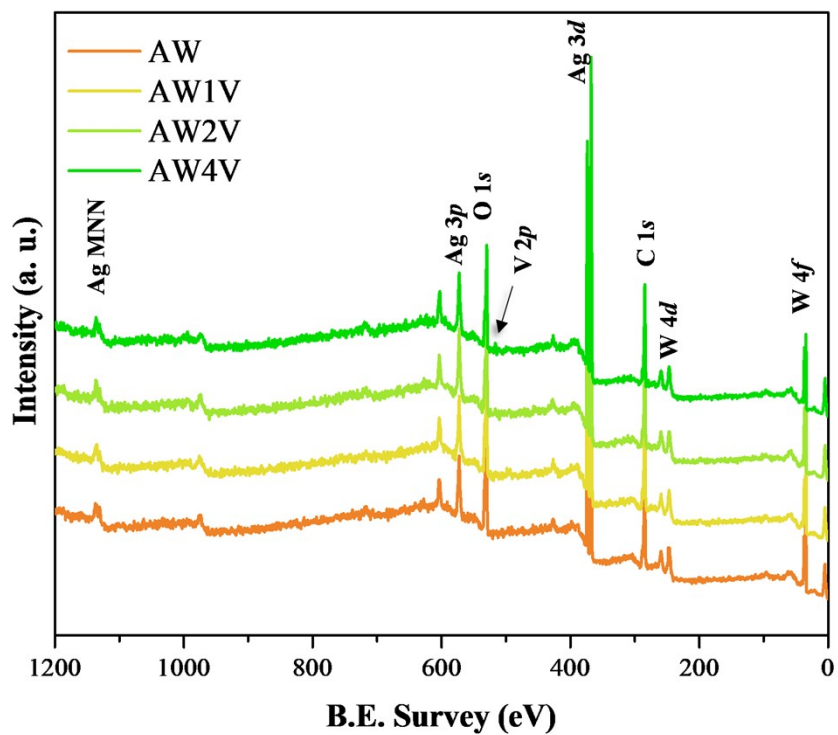


Figure SI-4. Survey XPS of the samples.

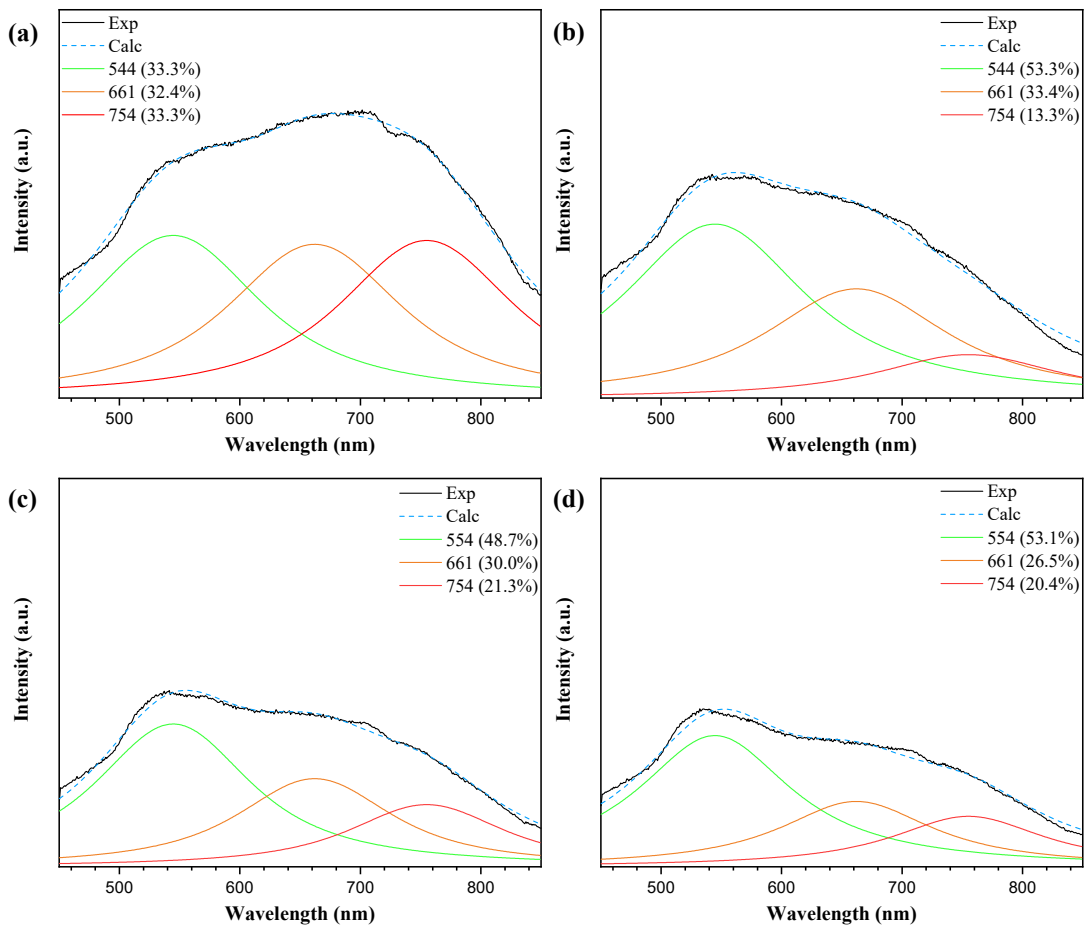


Figure SI-5. Deconvolution spectra of the (a) AW, (b) AW1V, (c) AW2V, and (d) AW4V samples.

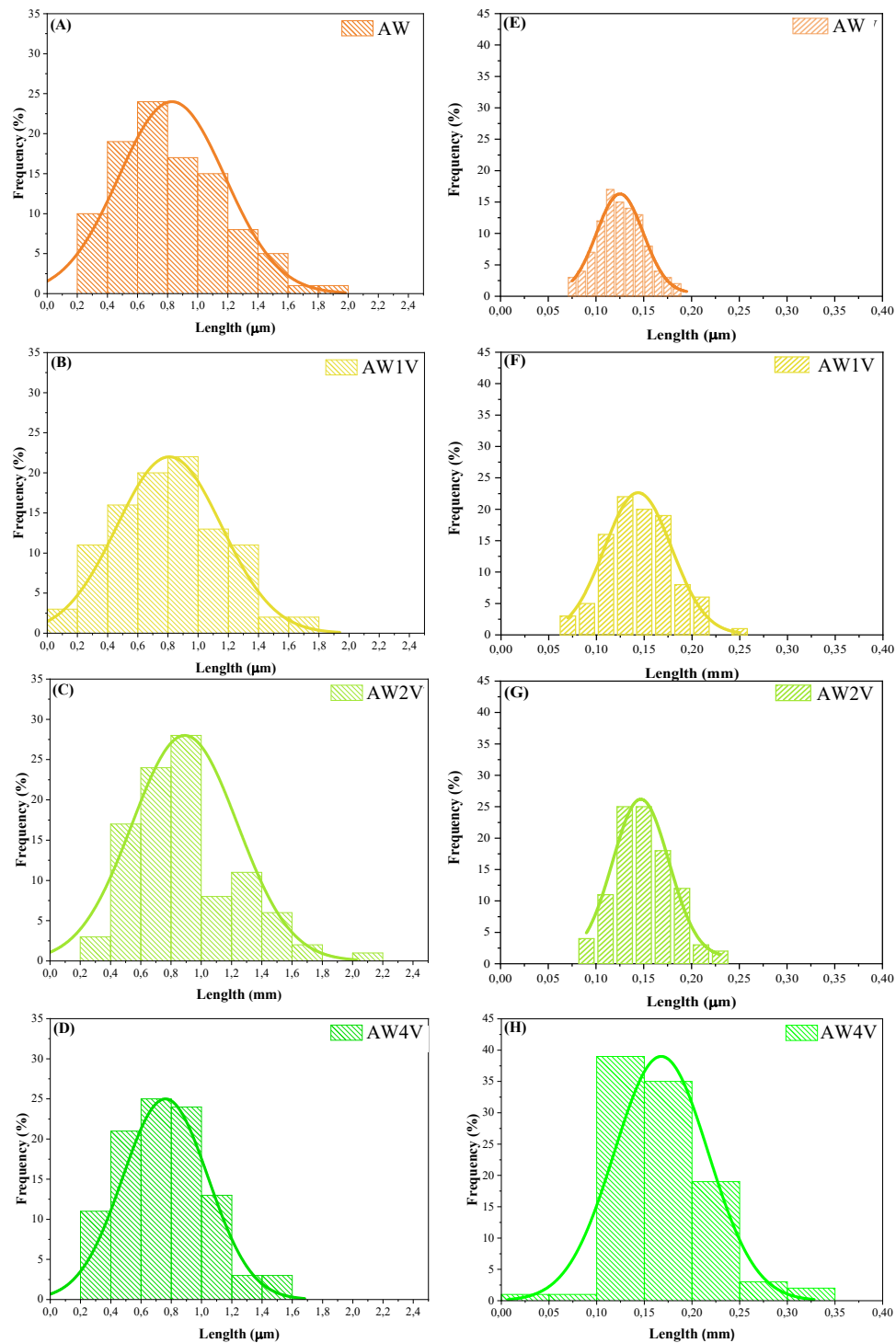


Figure SI-6. Average height (a-d) and width (e-h) distribution of AW and AWV samples.

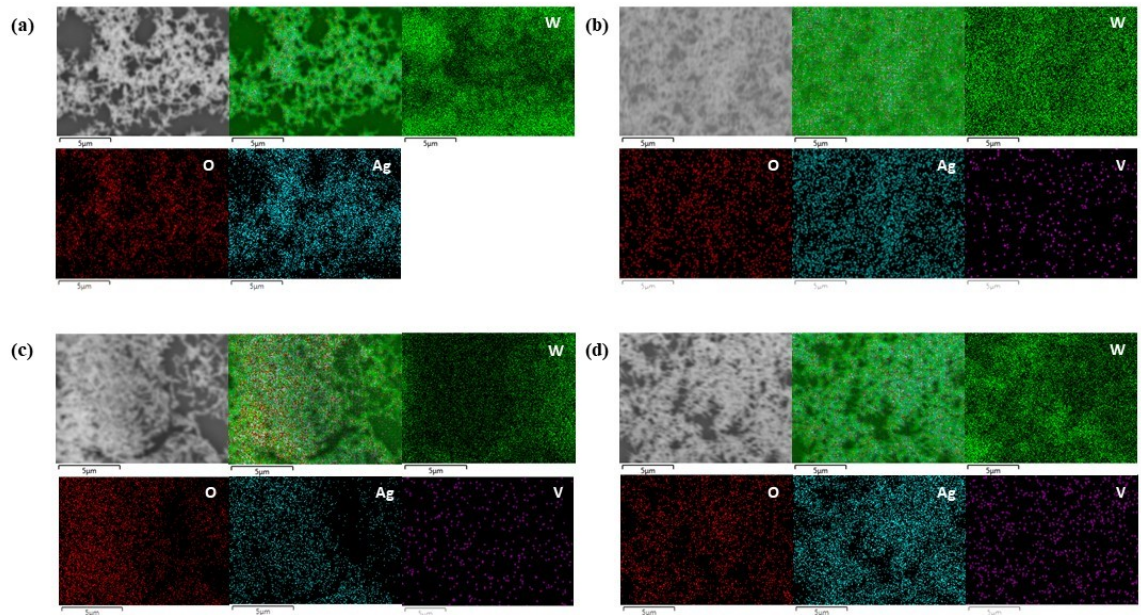


Figure SI-7. EDS mapping of the (a) AW, (b) AW1V, (c) AW2V, and (d) AW4V samples.

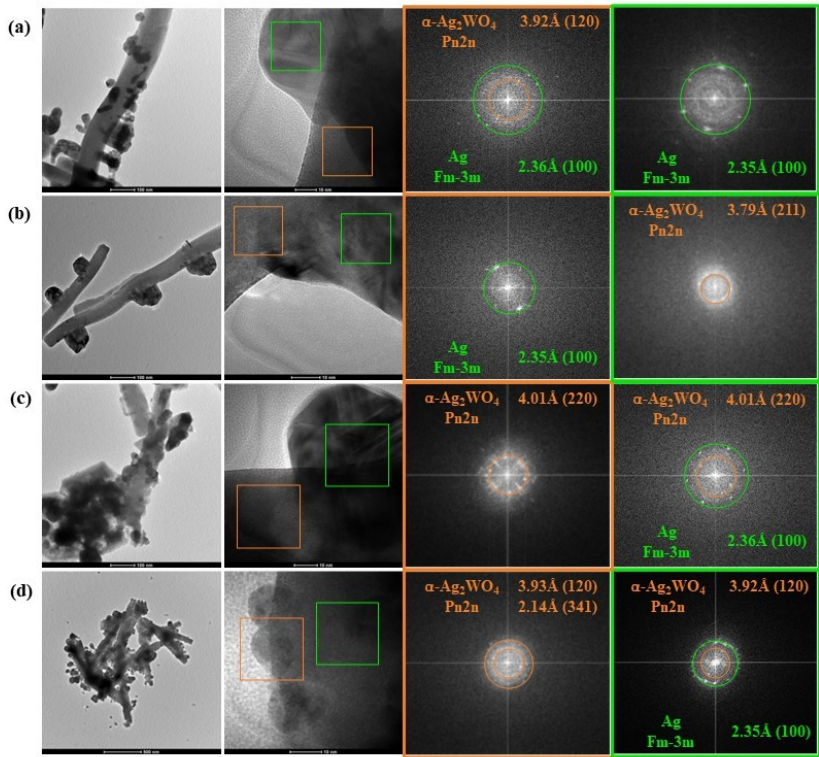


Figure SI-8. TEM images of (a) AW, (b) AW1V, (c) AW2V, and (d) AW4V samples.

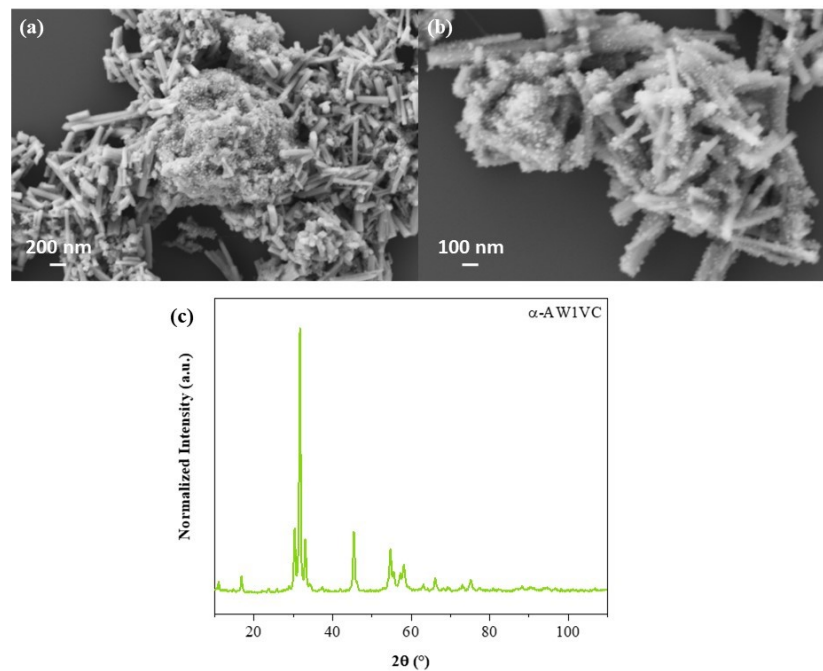


Figure SI-9. (a-b) SEM images and (c) XRD of the AW1V sample after the catalytic recycles.